

Characterization of clinafloxacin photodegradation products by LC-MS/MS and NMR

Michael J. Lovdahl *, Stephen R. Priebe

Analytical Development Department, Parke-Davis Pharmaceutical Research, Division of Warner-Lambert, 2800 Plymouth Road, Ann Arbor, MI 48105, USA

Received 17 December 1999; received in revised form 6 March 2000; accepted 7 March 2000

Abstract

Exposure of clinafloxacin to light results in photochemical degradation. The polar and nonpolar photodegradation products were profiled by HPLC using two sets of conditions. Clinafloxacin was subjected to severe light exposure conditions to obtain elevated levels of the photodegradation products for characterization. The structures of eight new degradation products were elucidated based on information from LC-MS/MS fragmentation and NMR spectra following isolation by preparative HPLC. Two photodegradation routes were identified: (1) dechlorination, followed by further reactions involving the quinolone ring, to yield polar photodegradation products; and (2) degradation of the pyrrolidine side-chain, yielding the nonpolar photodegradation products. © 2000 Elsevier Science B.V. All rights reserved.

Keywords: Photodegradation; Fluoroquinolones; LC-MS/MS; Structural characterization

1. Introduction

Clinafloxacin is a potent fluoroquinolone anti-infective drug with the structure shown in Fig. 1. Forced degradation studies conducted during development demonstrated that the compound is sensitive to light exposure both in solution and in the solid state, as has been reported for other quinolone type compounds such as ciprofloxacin [1,2]. The des-chloro analog of clinafloxacin, PD 124979, was readily identified by comparison of the HPLC retention time to that of authentic material. However, several unidentified polar

photodegradation products were observed by HPLC. Structural characterization of these impurities was of interest for understanding degradation mechanisms and interpretation of stability data. These photodegradation products may also occur under physiological conditions. Phototoxicity is a significant adverse effect of some quinolone-type antibacterial agents [3–5]. Two principal causes of the phototoxicity have been proposed; singlet oxygen [6–8], and the photogeneration of toxic reactive intermediates such as carbenes [9–11].

For quinolones containing a fluorine atom in the eight-position, defluorination has been demonstrated to be a significant photodegrada-

* Corresponding author. Tel.: +1-734-6227000.

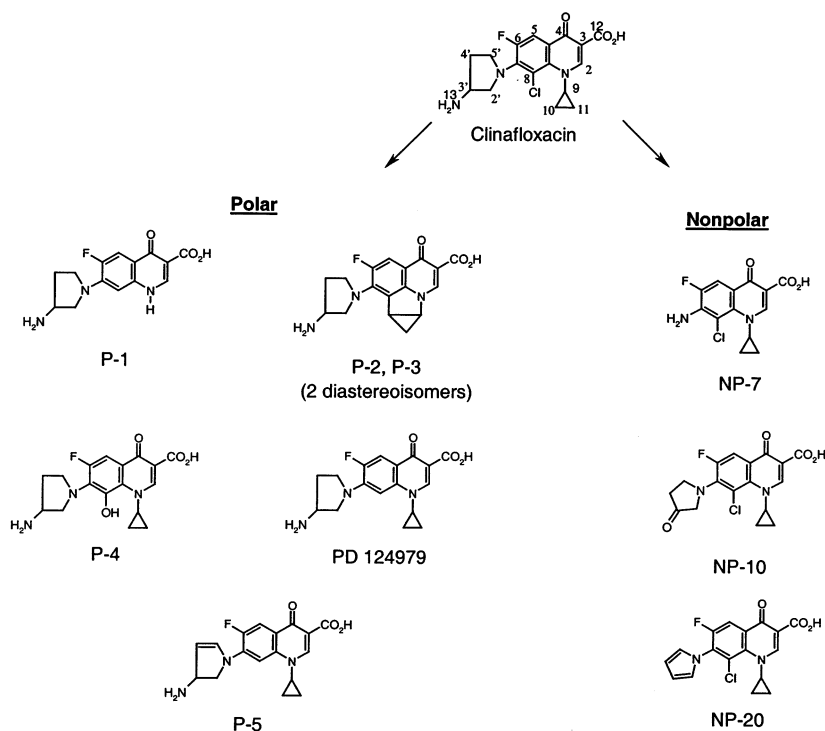


Fig. 1. Photodegradation products of clinafloxacin.

tion mechanism [9,12–16]. Piperazine ring opening followed by cleavage was observed for temafloxacin, along with oxidation of the secondary and tertiary amino groups [17]. Piperazine sidechain cleavage has also been observed for ciprofloxacin [18], norfloxacin [19], and enrofloxacin [20]. Clinafloxacin contains a chlorine atom in the eight-position and a 3-aminopyrrolidine sidechain.

A chromatogram of a sample exposed to simulated sunlight is provided in Fig. 2. It can be seen that four photodegradation product peaks (designated P-1, P-2, P-3, and P-4) eluting before PD 124979 are separated. The HPLC method was developed so as to provide complete separation of the photodegradants from each other and to be amenable to LC-MS analysis and preparative scale chromatography. When the photodegraded sample was analyzed using HPLC conditions incorporating higher proportion of organic solvent in the mobile phase, additional nonpolar photodegradation products were detected, as

shown in Fig. 3. The clinafloxacin samples subjected to light were initially characterized by LC-MS. Peaks of interest were purified by preparative HPLC using methods scaled from the analytical methods. The purified components were further characterized by NMR, where possible, and LC-MS/MS.

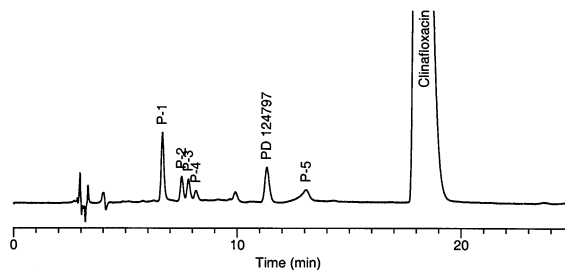


Fig. 2. Chromatogram of clinafloxacin degraded by exposure to simulated sunlight for 1 h in 1 N HCl, polar impurity profile method. HPLC conditions: column: YMC ODS-AQ, C_{18} , 5 μ m, 250 \times 4.6 mm; mobile phase: 0.1% formic acid/acetoneitrile (77:23); detection: 295 nm; flow rate: 1.0 ml min⁻¹; injection volume: 20 μ l; sample concentration: 1.0 mg ml⁻¹; diluent: mobile phase.

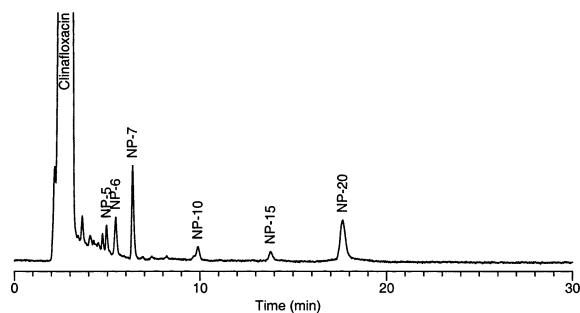


Fig. 3. HPLC chromatogram of clinafloxacin degraded under simulated sunlight for 2 h in 5% phosphoric acid, nonpolar impurity profile method. HPLC conditions: column: YMC ODS-AQ, C_{18} , 5 μ m, 250 \times 4.6 mm; mobile phase: 0.1% formic acid/acetonitrile (50:50); detection: 295 nm; flow rate: 1.0 ml min⁻¹; injection volume: 20 μ l; sample concentration: 1.0 mg ml⁻¹; diluent: mobile phase.

2. Experimental

2.1. Materials

Clinafloxacin hydrochloride Lot XP100996 was used as received from Parke-Davis Pharmaceutical Research (Ann Arbor, MI). All other reagents and solvents were of analytical or HPLC grade. The solid chemicals were purchased from E.

Merck (Darmstadt, Germany) and the solvents from Mallinckrodt (Paris, KY).

2.2. Apparatus

An Atlas Sunchex light chamber (Chicago, IL) providing simulated sunlight was used for forced degradation. The intensity was adjusted to 0.35 W m⁻² at 340 nm. Mass spectra were obtained using either a Micromass Platform II (Manchester, UK) single quadrupole mass spectrometer using atmospheric pressure chemical ionization or a Finnigan LCQ (San Jose, CA) ion trap mass spectrometer using electrospray ionization. NMR experiments were performed at ambient temperature on a Varian Unity Plus 400 (Palo Alto, CA) operating at 400 MHz. Analytical scale chromatography was performed using a Perkin-Elmer (Norwalk, CT) Series 200 LC pump, Series 200 autosampler, LC-235 diode array detector, and a YMC ODS-AQ column (Milford, MA), 250 \times 4.6 mm, 5- μ m particle size at ambient temperature. Preparative scale chromatography was performed using a Varian (Palo Alto, CA) Dynamax SD-1 solvent delivery system, SD-300 sample introduction pump, UV-1 detector, Isco (Lincoln, NE) Foxy

Table 1
LC-MS characterization of isolated photodegradation products

Photodegradation product	Retention time (min)	Apparent molecular weight ^a	Chlorine
<i>Polar</i>			
P-1	6.6	291	No
P-2	7.5	329	No
P-3	7.8	329	No
P-4	8.1	347	No
PD 124979	11.2	331	No
P-5	13.1	329	No
Clinafloxacin	18.1	365	Yes
<i>Nonpolar</i>			
Clinafloxacin	Void	365	Yes
NP-5	5	382	Yes
NP-6	6	368	Yes
NP-7	7	296	Yes
NP-10	10	364	Yes
NP-15	15	396	Yes
NP-20	20	346	Yes

^a Micromass Platform II, electrospray ionization for the polar method and atmospheric pressure chemical ionization for the nonpolar method.

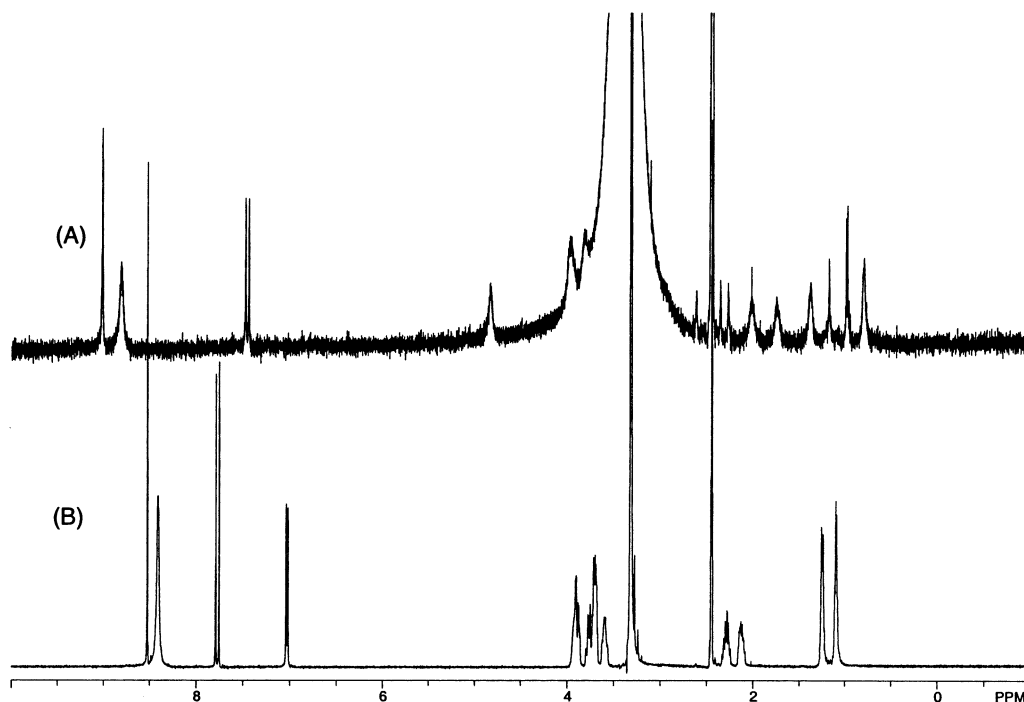


Fig. 4. ^1H NMR spectra of P-2 (A) and PD 124979 (B) in d^6 -DMSO. Note: peaks at 2.5 and 3.3 ppm are due to DMSO and water.

200 fraction collector, a YMC ODS-AQ 250×20 mm, $5\text{-}\mu\text{m}$ column at ambient temperature.

2.3. Photodegradation and purification of cinafloxacin degradation products

From preliminary photodegradation experiments, it was apparent that irradiation of low pH solutions of cinafloxacin with simulated sunlight would generate the desired products at elevated levels. An additional benefit of the use of low pH solutions was the increased solubility of cinafloxacin below pH 4. Two hours of exposure in a 5% phosphoric acid solution was chosen as a compromise between increasing levels of desired impurity formation, solubility of cinafloxacin, and further degradation to impurities not of interest. P-5 was the only photodegradant of interest not generated in significant quantities under these conditions.

Five grams of cinafloxacin were dissolved in 100 ml of 5% phosphoric acid solution. The solution was exposed to light in an open PyrexTM

beaker for 2 h. The resulting solution was adjusted to pH 5 with concentrated aqueous ammonia which is near the minimum solubility for cinafloxacin. The resulting suspension was filtered to remove the precipitated solids composed primarily of cinafloxacin as determined by HPLC assay. After filtering, the pH of the solu-

Table 2
 ^1H NMR assignments for PD 124979

Assignment	Number of H	Multiplicity	Shift (ppm)
12	1	S	15.4
2	1	S	8.52
13	2	S	8.4
5	1	D	7.77
8	1	D	7.02
9	1	M	3.89
3'	1	M	3.71
2'	2	M	3.87, 3.69
5'	2	M	3.76, 3.59
4'	2	M	2.28, 2.12
10, 11	4	M	1.24, 1.10

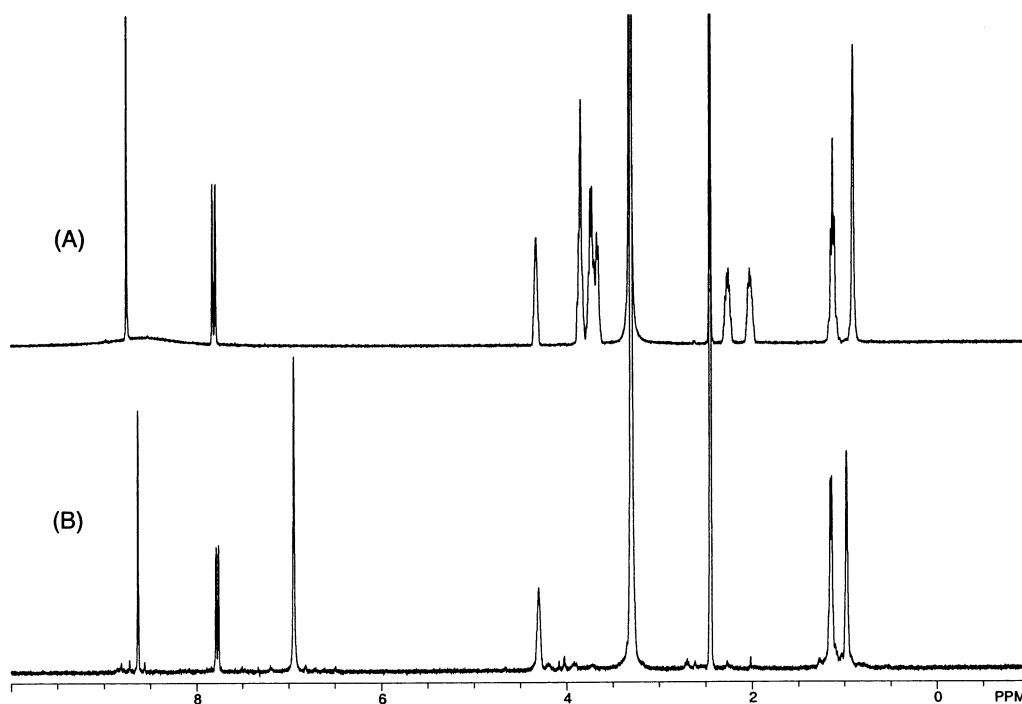


Fig. 5. ^1H NMR spectra of clinafloxacin (A) and NP-7 (B) in $\text{d}^6\text{-DMSO}$. Note: peaks at 2.5 and 3.3 ppm are due to DMSO and water.

tion was lowered to 2.5 with concentrated HCl to match the pH of the preparative mobile phase.

The liquor with enhanced levels of degradants was subjected to reversed-phase preparative chromatography by injecting 2 ml onto the preparative system. Mobile phase consisted of 0.1% formic acid/acetonitrile/methanol (75:15:10) at a flow rate of 10 ml min^{-1} . Eighteen 10-ml fractions were collected beginning at 100 ml of retention. Fractions corresponding to the peaks of interest were pooled. The pooled fractions were concentrated on a rotoevaporator to remove the acetonitrile and methanol prior to lyophilization.

2.4. LC-MS experiments

Samples were analyzed by atmospheric pressure chemical ionization in the positive ion mode over the mass range of 50–650 amu using the Micro-mass Platform II. The modified HPLC methods described above were used for sample introduction. Nitrogen was used at a flow rate of 450 l h^{-1}

for drying gas and 100 l h^{-1} for sheath gas. The source temperature was maintained at 110°C . A cone voltage of 25 V was used to determine m/z of the parent ion and isotope ratio. Increasing the cone voltage to as much as 75 V for some compounds induced in-source fragmentation of the parent ion.

To confirm the assigned structures of the polar impurities, LC-MS/MS experiments were per-

Table 3
 ^1H NMR assignments for clinafloxacin

Assignment	H	Shift (ppm)	Multiplicity
2	1	8.75	S
5	1	7.81	D
9	1	4.32	M
3'	1	3.84	M
2'	2	3.85, 3.74	M
5'	2	3.70, 3.66	M
4'	2	2.24, 2.02	M
10, 11	4	1.12, 0.90	M

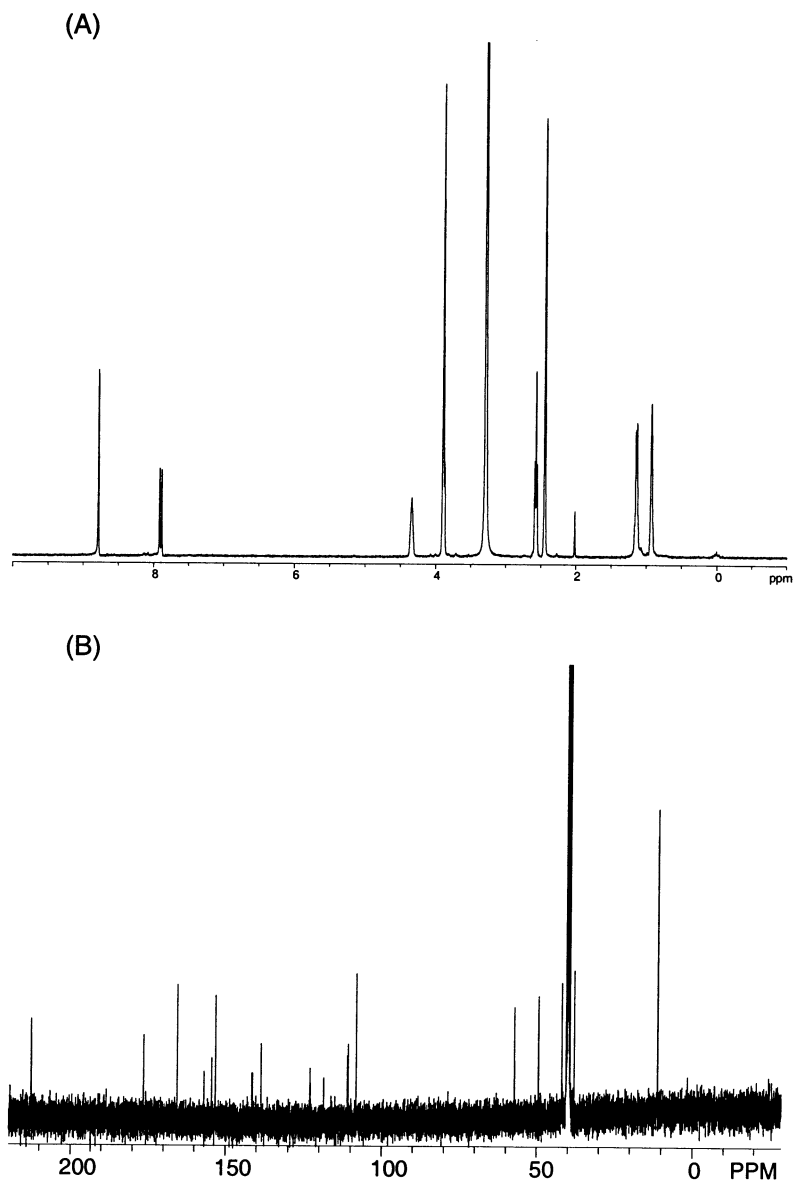


Fig. 6. ^1H NMR spectrum of NP-10 (A) ^{13}C NMR spectrum of NP-10 (B) in $^6\text{d-DMSO}$.

formed using the Finnigan LCQ ion trap system. The purified degradants were introduced using the HPLC methods described in Figs. 2 and 3 and analyzed by positive electrospray ionization with m/z scans from 50 to 400. The parent ion was selected and fragmented in an initial experiment.

The most prominent daughter ion was then selected and further fragmentation performed. The electrospray source voltage was held at 3.5 kV and the heated capillary maintained at 200°C . A capillary voltage of 5 V, tube lens offset of 15 V, and sheath gas flow at 28 l h^{-1} were used for all experiments.

Table 4
 ^1H -NMR assignments for NP-10

Assignment	H	Shift (ppm)	Multiplicity
2	1	8.79	S
5	1	7.90	D
9	1	4.34	M
2', 4'	4	3.88	M
5'	2	2.57	T
10, 11	4	1.14, 0.93	M

Table 5
 ^1H NMR assignments for NP-20

Assignment	H	Shift (ppm)	Multiplicity
2	1	8.87	S
5	1	8.17	D
2', 5'	2	6.98	M
3', 4'	2	6.31	M
9	1	4.34	M
10, 11	4	1.17, 1.09	M

2.5. NMR experiments

Typical experiments involved dissolving 3–5 mg of purified degradant in d_6 -DMSO and obtaining a ^1H NMR spectrum. Sixteen scans of each sample were taken at ambient temperature.

3. Results and discussion

The identified photodegradation products of cinafloxacin are summarized in Fig. 1. Numbering of the atoms follows the convention shown in Fig. 1 for all NMR references in the following sections.

3.1. LC-MS characterization

The severe photodegradation conditions resulted in the formation of four main polar products (Fig. 2) and several nonpolar peaks (Fig. 3). An additional photodegradation product, designated P-5, eluting just after PD 124979 was obtained by photodegradation in 1 N HCl (Fig. 2). LC-MS analysis of the purified components established the apparent molecular weight and the presence or absence of chlorine. The presence or absence of chlorine was ascertained by examination of the apparent molecular ion peak for the characteristic isotope ratio. This information is summarized in Table 1. The polar photodegradation products 1–5 did not contain chlorine. The

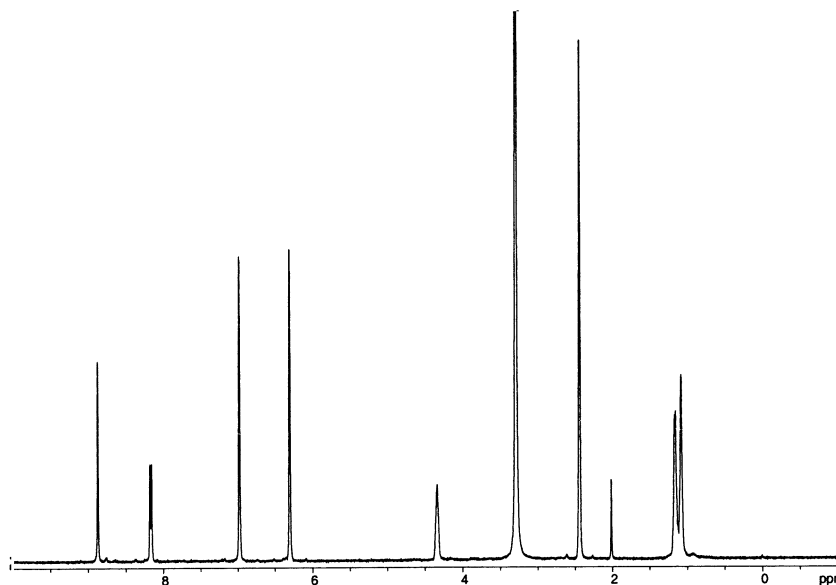


Fig. 7. ^1H NMR spectrum of NP-20 in d_6 -DMSO.

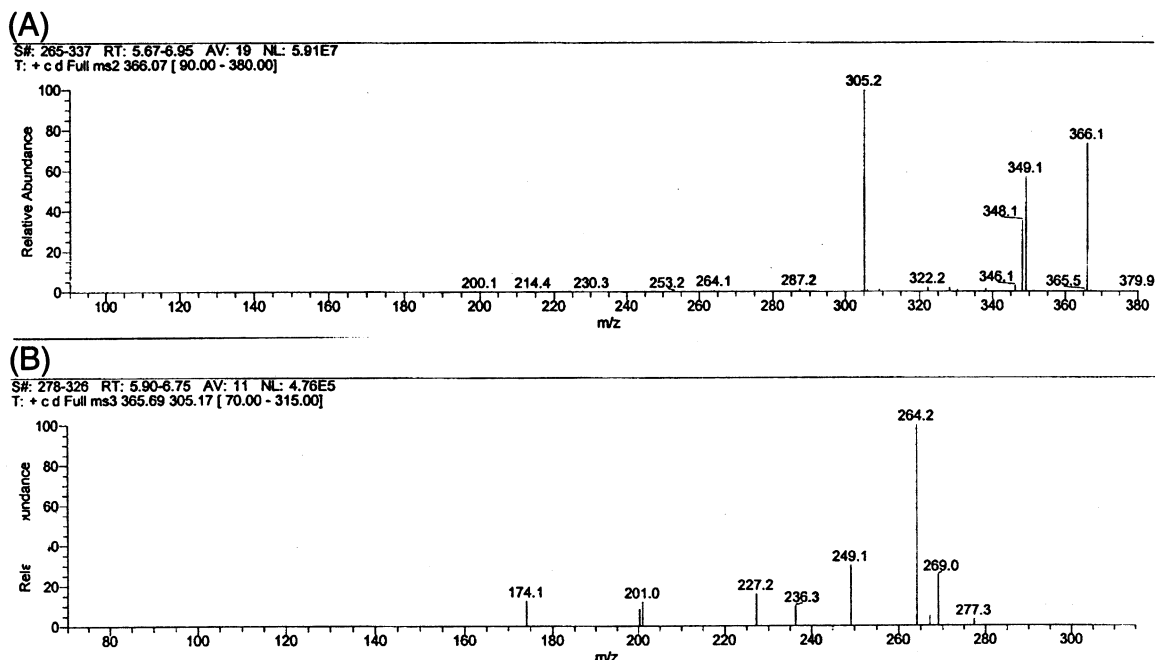


Fig. 8. Mass spectra of clinafloxacin (A) and m/z 305 ion (B).

mass of polar photodegradation product 1 (P-1) was 40 amu lower than that of PD 124979, which is consistent with loss of the cyclopropyl moiety. P-2 and P-3 exhibited a mass two units lower than PD 124979, suggesting formation of an additional bond. P-4, with an apparent molecular mass of 347, could be explained by the addition of $-\text{OH}$. P-5 gave a molecular mass 2 amu less than PD 124979, again indicating possible formation of another bond. When P-5 underwent in-source fragmentation by increasing the cone voltage, the pattern was analogous to that of PD 124979 for those fragments containing the pyrrolidine sidechain except for a 2 amu mass difference. This information indicated that the additional bond was present on the pyrrolidine sidechain. Difficulties were encountered in the isolation of a sufficient quantity of P-5 for NMR analysis due to instability. P-5 further degraded to lesser components upon attempts at isolation and this product was not characterized further.

The nonpolar photodegradation products did not exhibit loss of chlorine. The NP-7, NP-10, and NP-20 peaks were selected for further study

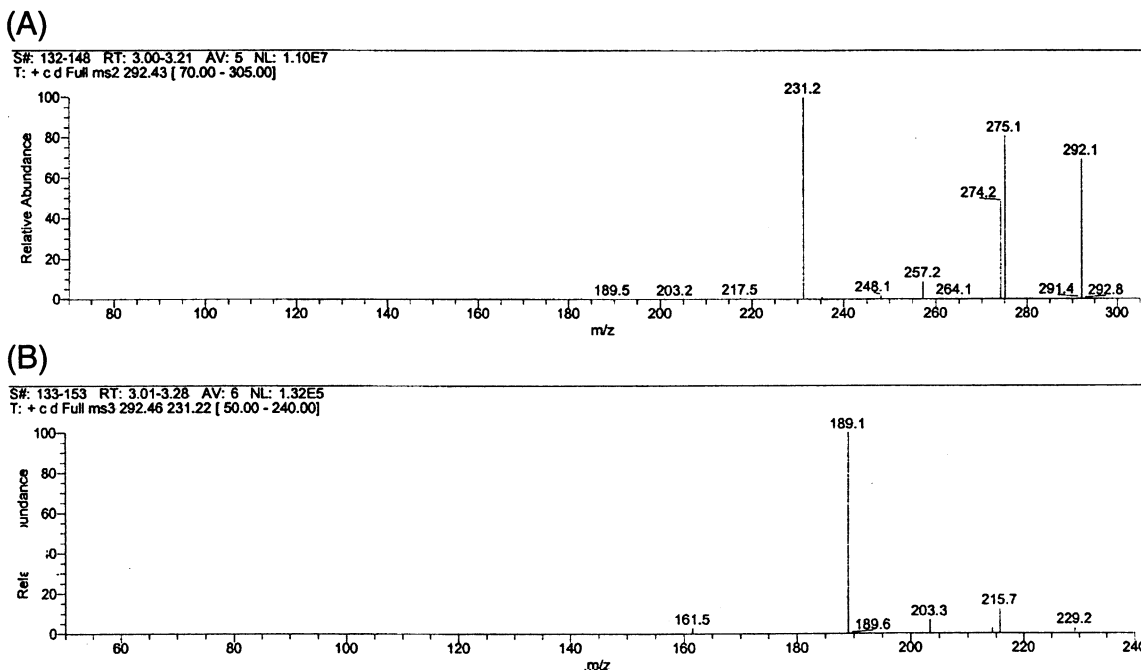
on the basis of the ease of isolation in sufficient purity and their occurrence in light stability samples. Other nonpolar photodegradation peaks below 0.1 area percent in light stability samples were not considered for characterization.

Table 6

Ion structure assignments for clinafloxacin^a

Ion (m/z)	Structural assignment
366	$[\text{M} + \text{H}]^+$
349	$[\text{M} - \text{NH}_3 + \text{H}]^+$
348	$[\text{M} - \text{H}_2\text{O}]^+$
346	$[\text{M} - \text{HF} + \text{H}]^+$
322	$[\text{M} - \text{CO}_2 + \text{H}]^+$
305	$[\text{M} - \text{H}_2\text{O} - \text{C}_2\text{H}_5\text{N}]^+$
277	$[\text{D}_{305} - \text{CO}]^+$
269	$[\text{D}_{305} - \text{HCl}]^+$
264	$[\text{D}_{305} - \text{C}_2\text{H}_3\text{N}]^+$
249	$[\text{D}_{305} - \text{HCl} - \text{HF}]^+$
236	$[\text{D}_{305} - \text{C}_2\text{H}_3\text{N} - \text{CO}]^+$
227	$[\text{D}_{305} - \text{HCl} - \text{CH}_2 - \text{CO}]^+$
200	$[\text{D}_{305} - \text{HCl} - \text{C}_2\text{H}_3\text{N} - \text{CO}]^+$
174	$[\text{D}_{305} - \text{HCl} - \text{C}_2\text{H}_3\text{N} - \text{CO} - \text{C}_2\text{H}_2]^+$

^a M, molecular ion; D_n, a daughter ion source.

Fig. 9. Mass spectra of P-1 (A) and m/z 231 ion (B).

3.2. NMR

3.2.1. P-2

A 7-mg quantity of P-2 was isolated in 87% (area) purity when assayed by the modified polar method at 295 nm. The ^1H NMR spectrum of P-2 is compared to that of PD 124979 in Fig. 4. The proton assignments for PD 124979 are listed in Table 2.

Although the quality of the P-2 spectrum is degraded by the presence of water and impurities, several key features can be identified. In the aromatic region (7–9 ppm), it can be seen that the proton at the eight-position of PD 124979 is absent in the spectrum of P-2. As seen in the PD 124979 spectrum and Table 2, the cyclopropyl group gives rise to several distinctive signals. These are altered in the spectrum of P-2, suggesting formation of a bond from the cyclopropyl group to the eight-position of the quinolone ring. The proposed structure of P-2 is shown in Fig. 1. An analogous photodegradation product has been reported for the structurally related fluoroquinolone lomefloxacin [12].

P-3 exhibits the same apparent molecular mass as P-2, an identical mass spectral fragmentation pattern, and elutes very closely in the HPLC impurity profile. P-3 is, therefore, proposed to be a stereoisomer of P-2. Clinafloxacin is racemic at the chiral site on the pyrrolidine ring and, therefore, formation of a second chiral center in the proposed structure for P-2 would be expected to result in a pair of diastereoisomers.

Table 7
 Ion structure assignments for P-1^a

Ion (m/z)	Structural assignment
292	$[\text{M} + \text{H}]^+$
275	$[\text{M} - \text{NH}_3 + \text{H}]^+$
274	$[\text{M} - \text{H}_2\text{O}]^+$
257	$[\text{M} - \text{NH}_3 - \text{H}_2\text{O}]^+$
248	$[\text{M} - \text{CO}_2 + \text{H}]^+$
231	$[\text{M} - \text{H}_2\text{O} - \text{C}_2\text{H}_5\text{N}]^+$
215	$[\text{D}_{231} - \text{CH}_2 - \text{H}_2]^+$
203	$[\text{D}_{231} - \text{CO}]^+$
189	$[\text{D}_{231} - \text{CO} - \text{CH}_2]^+$

^a M, molecular ion; D_n , a daughter ion source.

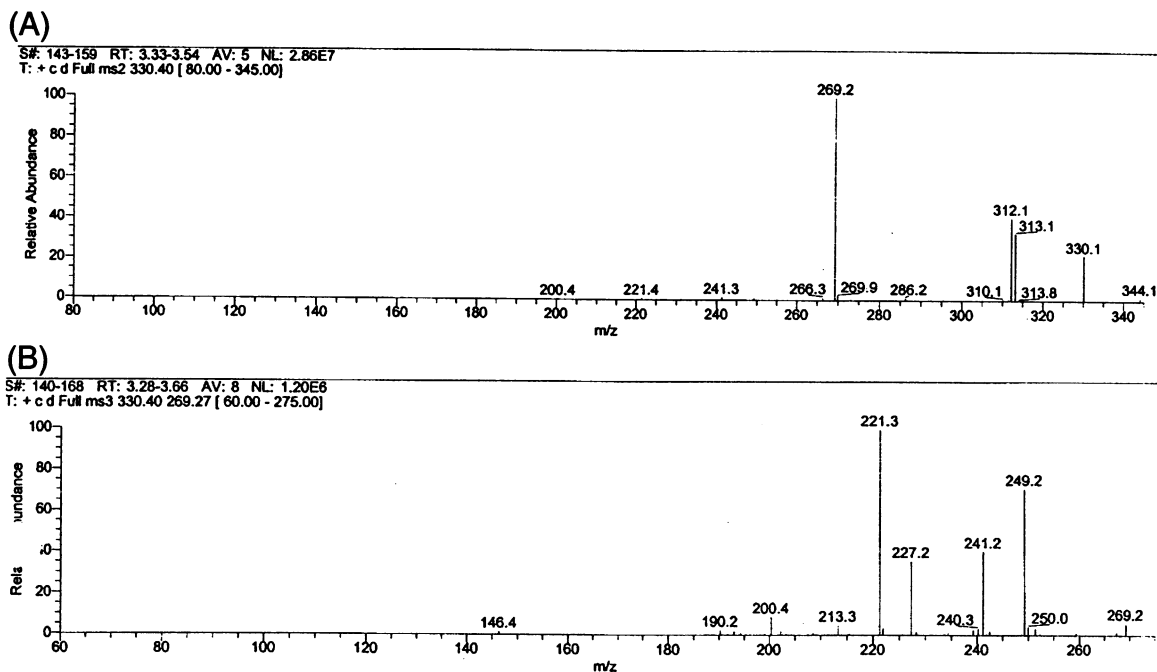


Fig. 10. Mass spectra of P-2 (A) and m/z 269 ion (B).

3.2.2. NP-7

An 18-mg quantity of NP-7 was isolated in 87% (area) purity when assayed by the nonpolar impurity profile method at 295 nm. The ^1H NMR spectrum is shown in Fig. 5B. This spectrum may be compared to that of cinafloxacin obtained under the same conditions (Fig. 5A). The spectral assignments for cinafloxacin are listed in Table 3.

Several key differences are apparent in the spectrum of NP-7. All pyrrolidine resonances are absent. The quinolone aromatic proton signals seen for cinafloxacin remain, with minor shifts. A new resonance in the spectrum of NP-7 at 6.9 ppm integrating as two protons may be assigned to an amino group at the seven-position. These observations, and the apparent molecular mass observed by LC-MS, are consistent with the loss of the pyrrolidine ring but retention of the ring nitrogen. The structure of NP-7 is shown in Fig. 1.

This compound had previously been synthesized and was available in the Parke-Davis compound library as PD 156595. Comparison of the ^1H NMR spectrum with that of the authentic material afforded a positive match. In addition,

the retention time of authentic PD 156595 matched that of NP-7.

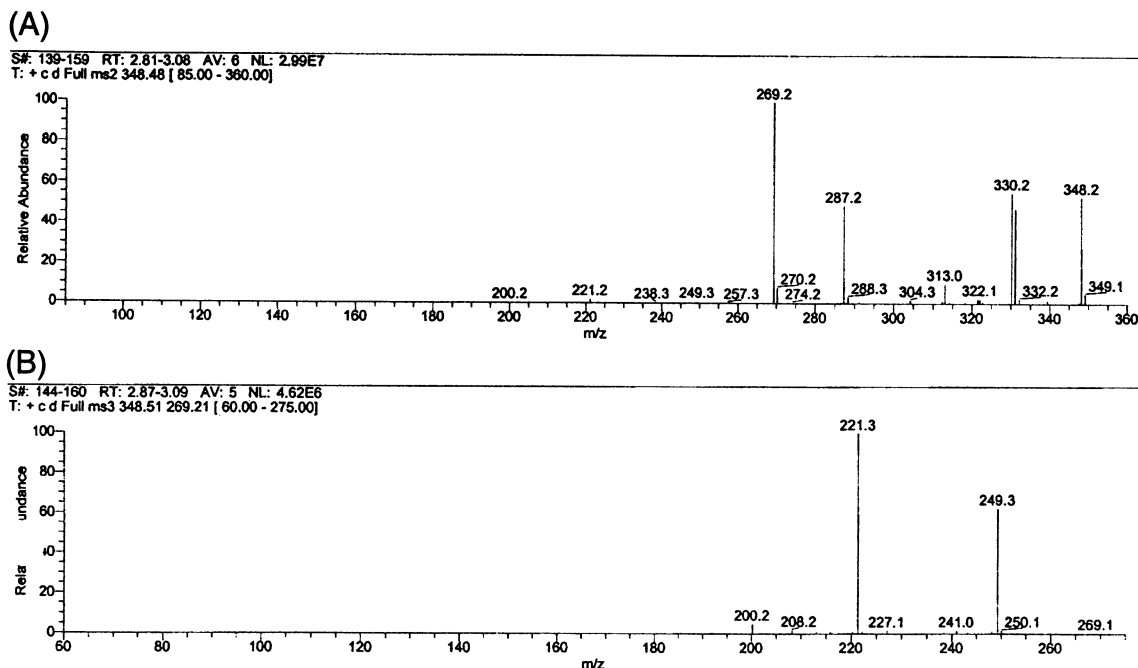
3.2.3. NP-10

A 52-mg quantity of NP-10 was isolated in 98% (area) purity when assayed by the nonpolar impurity profile method at 295 nm. The ^1H NMR spectrum is shown in Fig. 6A. This spectrum

Table 8
Ion structure assignments for P-2^a

Ion (m/z)	Structural assignment
330	$[\text{M} + \text{H}]^+$
313	$[\text{M} - \text{NH}_3 + \text{H}]^+$
312	$[\text{M} - \text{H}_2\text{O}]^+$
286	$[\text{M} - \text{CO}_2 + \text{H}]^+$
269	$[\text{M} - \text{H}_2\text{O} - \text{C}_2\text{H}_5\text{N}]^+$
249	$[\text{D}_{269} - \text{HF}]^+$
241	$[\text{D}_{269} - \text{CO}]^+$
227	$[\text{D}_{269} - \text{CO} - \text{CH}_2]^+$
221	$[\text{D}_{269} - \text{CO} - \text{HF}]^+$
200	$[\text{D}_{269} - \text{CO} - \text{C}_2\text{H}_5\text{N}]^+$

^a M, molecular ion; D_n, a daughter ion source.

Fig. 11. Mass spectra of P-4 (A) and m/z 269 ion (B).

shows key differences in the pyrrolidine region (2.0–2.3 and 3.6–3.9 ppm), when compared to the spectrum of cinafloxacin (Fig. 5A). A new set of signals now appears at 2.6 and 3.9 ppm. The quinolone protons remain present as in the spectrum of cinafloxacin, with minor shifts. The ^{13}C NMR spectrum acquired from the same sample is shown in Fig. 6B. Resonances at 165, 176, and 212 ppm are indicative of carbonyl carbons. The IR spectrum (not shown) displayed a strong band at 1759 cm^{-1} not seen in the spectrum of cinafloxacin, which is in the frequency range expected for absorption by a cyclic ketone in a five-member ring. This evidence, coupled with the apparent molecular weight of 365, is consistent with the structure in Fig. 1 and assignments listed in Table 4.

3.2.4. NP-20

A 50-mg quantity of NP-20 was isolated in 92% (area) purity when assayed by the nonpolar impurity profile method at 295 nm. The ^1H NMR spectrum in Fig. 7 shows changes in the pyrrolidine region, compared to the spectrum of

clinafloxacin (Fig. 5A). New peaks appear at 6.3 and 7.0 ppm, with a total of four protons, which corresponds to the pyrrole structure shown in Fig. 1 and proton assignments listed in Table 5.

This compound had been synthesized previously and was available in the Parke-Davis compound library as PD 156597. Comparison of the

Table 9
Ion structure assignments for P-4^a

Ion (m/z)	Structural assignment
348	$[\text{M} + \text{H}]^+$
331	$[\text{M} - \text{NH}_3 + \text{H}]^+$
330	$[\text{M} - \text{H}_2\text{O}]^+$
313	$[\text{M} - \text{NH}_3 - \text{H}_2\text{O}]^+$
304	$[\text{M} - \text{CO}_2 + \text{H}]^+$
287	$[\text{M} - \text{H}_2\text{O} - \text{C}_2\text{H}_5\text{N}]^+$
269	$[\text{M} - \text{H}_2\text{O} - \text{C}_2\text{H}_5\text{N} - \text{H}_2\text{O}]^+$
249	$[\text{D}_{269} - \text{HF}]^+$
241	$[\text{D}_{269} - \text{CO}]^+$
227	$[\text{D}_{269} - \text{CO} - \text{CH}_2]^+$
221	$[\text{D}_{269} - \text{CO} - \text{HF}]^+$
200	$[\text{D}_{269} - \text{CO} - \text{C}_2\text{H}_5\text{N}]^+$

^a M, molecular ion; D_n, a daughter ion source.

Table 10

Summary of fragmentation for parent ions of clinafloxacin and photodegradation products 1–4^{a1}

Compound	Ion assignment/mass					
	M + H ⁺	M–NH ₃ + H ⁺	M–H ₂ O	M–CO ₂ + H ⁺	M–H ₂ O–C ₂ H ₅ N	Other
Clinafloxacin	366	349	348	322	305 (100)	
P-1	292	275	274	248	231 (100)	257 ^{b1}
P-2, P-3	330	313	312	286	269 (100)	
P-4	348	331	330	304	287	313 ^{b1} , 269 (100) ^{c1}

^a The most intense ion is indicated by (100).^b M–NH₃–H₂O.^c M–H₂O–C₂H₅N–H₂O.

Table 11

Second generation product ions fragmentation^{a1}

Compound	Ion assignment/mass					
	Precursor ion ^{b1}	D _n –HF	D _n –CO	D _n –CO–CH ₂	D _n –CO–C ₂ H ₅ N	Other
Clinafloxacin	305	249 ^{c1}	277	227 ^{d1}	236, 200 ^{e1}	269 ^{f1} , 264 (100) ^{g1}
P-1	231	–	203	189 (100)	–	215 ^{h1}
P-2, P-3	269	249	241	227	200	221 (100) ⁱ¹
P-4	269 ^{j1}	249	241	227	200	221 (100) ⁱ¹

^a The most intense ion is indicated by (100).^b M–H₂O–C₂H₅N.^c D₃₀₅–HCl–HF.^d D₃₀₅–HCl–CO–CH₂.^e D₃₀₅–HCl–CO–C₂H₅N.^f D₃₀₅–HCl.^g D₃₀₅–C₂H₅N.^h D₂₃₁–NH₂.ⁱ D₂₆₉–CO–HF.^j M–H₂O–C₂H₅N–H₂O.

¹H NMR spectrum obtained from the isolated material with a reference spectrum gave a positive match. Injection of authentic PD 156597 produced a peak with the same retention time as the NP-20 peak from the photodegraded material.

3.3. LC-MS/MS

3.3.1. Clinafloxacin

To provide a reference data set, the clinafloxacin peak was analyzed first by selection of the parent ion at 366 *m/z* and fragmentation, and then by selection of the most prominent fragment (305 *m/z*) and subjecting this ion to further fragmentation (mass spectra shown in Fig.

8). The assignment of the observed masses is listed in Table 6. The assignments were guided by available literature for other quinolones [10].

3.3.2. P-1

The mass spectra observed for P-1 are shown in Fig. 9 and the assignments are listed in Table 7. The fragmentation pattern was analogous to that seen for clinafloxacin (Fig. 8), for the most part, and supports the assigned structure (Fig. 1). The minor ion with *m/z* 257, corresponding to loss of both NH₃ and H₂O, was not observed in the spectrum of clinafloxacin. In the daughter ion (*m/z* 231) spectrum, the most intense ion (*m/z* 189) corresponds to loss of CO from the

quinolone ring and CH_2 from the sidechain. This was a minor ion in the spectrum of the corresponding cinafloxacin daughter ion (m/z 305).

3.3.3. P-2

The mass spectra observed for P-2 are shown in Fig. 10 and the fragment ion assignments listed in Table 8. The fragmentation pattern was analogous to that seen for cinafloxacin and supports the structure proposed above. The fragmentation pattern (data not shown) observed for P-3 was essentially the same as that of P-2 and again analogous to that seen for cinafloxacin. P-3 is proposed to be a stereoisomer of P-2.

3.3.4. P-4

The mass spectra observed for P-4 are shown in Fig. 11 and the ion structure assignments are listed in Table 9. The spectra were similar to those seen for cinafloxacin and support the structure in which the chlorine is replaced with a hydroxyl group. However, in this case the $\text{M}-\text{H}_2\text{O}-\text{C}_2\text{H}_5\text{N}$ peak at m/z 287 was not the most intense fragment. Loss of the 8-hydroxyl group with ring formation resulted in m/z 269 fragment which exhibited the highest intensity. This is the same daughter ion as seen for P-2 and P-3, and it gave the same fragmentation pattern. The ion with m/z 313, corresponding to loss of both NH_3 and H_2O , was not observed at significant intensity in the spectra of cinafloxacin or P-2 or P-3, but the corresponding ion was seen in P-1.

3.3.5. Summary of LC-MS/MS data

The fragmentation of the parent molecular ions is summarized in Table 10. For this series of compounds loss of water, along with ring contraction of the pyrrolidine sidechain, is a significant pathway leading to the most intense fragment ion. In the case of P-4, the most intense ion resulted from an additional dehydration coupled with ring formation.

The fragmentation of the second-generation product ions obtained from the most intense ion of the parent spectrum is summarized in Table 11. Differences were seen between compounds in the occurrence and intensity of fragments. All precursor ions exhibited fragments arising from loss of

CO from the quinolone ring and CH_2 from the pyrrolidine sidechain. $\text{D}-\text{CO}-\text{CH}_2$ was the most intense product peak in the case of P-1. Loss of the entire sidechain was favored for cinafloxacin (m/z 264 [100]) and occurred to a small extent, along with loss of CO, for the m/z 269 precursor ion of P-2, P-3, and P-4 to produce an m/z 200 fragment. Loss of HF and CO from the D_{269} ion led to the most intense product ion for P-2, P-3, and P-4.

4. Conclusions

The identified photodegradation products of cinafloxacin are summarized in Fig. 1. The polar compounds are dechlorinated with further degradation associated with the quinolone or pyrrolidine ring. P-2, P-3, and P-4 are products expected from a reactive intermediate formed by loss of chlorine, such as a carbene [13]. An additional polar degradation product, P-5, retention time 5.9 min, exhibits an apparent molecular weight of 329, does not contain chlorine, and has a unit of unsaturation on the pyrrolidine ring. The nonpolar photodegradation peaks represent side-chain degradation without loss of chlorine. Three additional nonpolar photodegradation products (NP-5, NP-6, and NP-15) were partially characterized. The information gathered during this study was useful for the evaluation of light stability studies and phototoxicity.

References

- [1] G. Phillips, B.E. Johnson, J. Ferguson, J. Antimicrob. Chemother. 26 (1990) 783–789.
- [2] K. Torniaainen, S. Tammilehto, V. Ulvi, Int. J. Pharm. 132 (1996) 53–61.
- [3] J. Ferguson, Photochem. Photobiol. 62 (1995) 954–958.
- [4] P. Ball, G. Tillotson, Drug Safety 13 (1995) 343–358.
- [5] P.S. Lietman, Drugs 49 (1995) 794–850.
- [6] R. Baran, P. Brun, Dermatologia 173 (1986) 85–188.
- [7] D. Robertson, G. Epling, J. Keily, D. Bailey, B. Song, Toxicol. Appl. Pharmacol. 111 (1991) 221–232.
- [8] N. Umezawa, K. Arakane, A. Ryn, S. Maskiko, M. Hirobe, T. Nagano, Arch. Biochem. Biophys. 342 (2) (1997) 275–281.

- [9] E. Fasani, A. Profumo, A. Albini, *Photochem. Photobiol.* 68 (1998) 666–674.
- [10] D.A. Volmer, B. Mansoori, S.J. Locke, *Anal. Chem.* 69 (1997) 4143–4155.
- [11] S.R. Norby, P.S. Lietman, *Drugs* 45 (Suppl. 3) (1993) 59–64.
- [12] E. Fasani, M. Mella, D. Caccia, S. Tassi, M. Fagnoni, A. Albini, *Chem. Commun.* (1997) 1329–1330.
- [13] L.J. Martinez, G. Li, C.F. Chignell, *Photochem. Photobiol.* 65 (1997) 599–602.
- [14] G. Condorelli, G. De Guidi, S. Giuffrida, P. Miano, A. Velardita, S. Sortino, *Photochem. Photobiol.* 63 (1996) 75S.
- [15] T. Morimura, T. Nobuhara, H. Matsukura, *Chem. Pharm. Bull.* 45 (1997) 373–377.
- [16] M. Engler, G. Rusing, F. Sorgel, U. Holzgrabe, *Antimicrob. Agents Chemother.* 42 (1998) 1151–1159.
- [17] L. Elrod, C.L. Linton, B.P. Shelat, C.F. Wong, *J. Chromatogr.* 519 (1990) 125.
- [18] K. Torniaainen, J. Mattinen, C.-P. Askolin, S. Tammilehto, *J. Pharm. Biomed. Anal.* 15 (1997) 887–894.
- [19] A. Nangia, F. Lam, C.T. Hung, *Drug Dev. Ind. Pharm.* 17 (1991) 681–694.
- [20] J. Burhenne, M. Ludwig, M. Spiteller, *Chemosphere* 38 (1999) 1279–1286.